NUCET NUCLEAR ENERGY AND TECHNOLOGY

Nuclear Energy and Technology 7(2): 157–164
DOI 10.3897/nucet.7.60122

Research Article

Development and characterization of a mobile γ spectrometer and its field deployment for in situ radioactivity measurements

T. J. Mertzimekis[1], C. Andrikopoulos[1], C. Fakiola[1], A. Kotsovolou[1], D. Lampridou[2], S. Kazana[2]

1 *Department of Physics, National and Kapodistrian University of Athens, Zografou Campus, GR-15784, Athens, Greece*

2 *Department of Geology & Geoenvironment, National and Kapodistrian University of Athens, Zografou Campus, GR-15784, Athens, Greece*

Corresponding author: T. J. Mertzimekis (tmertzi@phys.uoa.gr)

Academic editor: Sergey Ulin ♦ **Received** 28 October 2020 ♦ **Accepted** 15 June 2021 ♦ **Published** 24 June 2021

Citation: Mertzimekis TJ, Andrikopoulos C, Fakiola C, Kotsovolou A, Lampridou D, Kazana S (2021) Development and characterization of a mobile γ spectrometer and its field deployment for in situ radioactivity measurements. Nuclear Energy and Technology 7(2): 157–164. https://doi.org/10.3897/nucet.7.60122

Abstract

A mobile γ–ray spectrometer (*AMESOS*) has been developed using a 3"×3" NaI(Tl) detector, a custom–made mounting holder, and portable electronics to perform *in situ* measurements of radioactivity. The spectrometer was calibrated using standard point sources and its absolute efficiency was determined. As a field test operation, AMESOS was deployed on the premises of the University of Athens Zografou campus focusing on estimating the NORM levels. Data were analyzed and used to create radiological maps for the metropolitan UoA campus for the first time. Besides natural radioactivity levels, trace concentrations of ^{137}Cs were also detected, attributed to the Chernobyl fallout in Greece. An overall steady performance of the spectrometer was observed throughout the field operation. AMESOS is ready to be deployed for *in situ* studies of environmental radioactivity and radwaste management.

Keywords

AMESOS, environmental radioactivity, mobile spectrometer, radiological map

Introduction

Mobile γ–ray spectrometry is a well–established technique in environmental radioactivity measurements, which can provide results in harsh or remote environments (ICRU 1994), especially when sampling is difficult or when information is needed in a very short time scale. Nowadays mobile spectrometers are rather simple to deploy in the field and can be carried by humans (Kock and Samuelsson 2011, Cresswell et al. 2013, 2018), mounted on robotic instruments (Jilek et al. 2016), air vehicles (Simon and Graham 1998, Kock and Samuelsson 2011), drones (Kurvinen et al. 2005, Pöllänen et al. 2009), or dive into deep oceans aboard marine submersibles (Hattori 2000, Hattori et al. 2001, Tsabaris et al. 2011, Androulakaki et al. 2016). Depending on the application, different types of detectors can be used, such as scintillators (e.g. NaI(Tl)) or solid–state detectors (e.g. HPGe), coupled to integrated electronics modules for data acquisition or custom–made designs to accommodate special needs. The major drawback of mobile systems has been the limitations in supplying stable, uninterrupted power, which generally shortens the duration of measurements in the field. However, as technology leaps forward, power autonomy becomes less and less of an issue, thus extending the range of applications where a mobile spectrometer can be exploited.

Scintillators are typically favored over solid–state detectors (Ge(Li) or HPGe) for mobile spectrometers, since the latter traditionally require cooling with liquid nitrogen to operate, are generally more expensive, and are overall more sensitive in field deployment, despite the higher resolution they offer (Clouvas et al. 2004). On the other hand, scintillators are sensitive to environmental conditions, especially temperature changes that may cause gain shifts during operation (Gilmore 2008).

In any case, a careful characterization of the spectrometer is required, especially in terms of its absolute efficiency. The response function of the spectrometer depends on the type of the detector, the geometrical characteristics of the spectrometer and the energies of the photons emitted by the isotopes of interest. Standard point sources are typically used for γ–ray spectrometers, but for mobile systems aiming at measurements in wide–open areas, a characterization under realistic conditions is often additionally necessary.

In this paper, a mobile spectrometer, *AMESOS*: A MobilE Spectrometer for environmental radioactivity Studies[1], has been developed in the National and Kapodistrian University of Athens (UoA) to support a basic program of *in situ* environmental radioactivity measurements (see photo of the actual setup in Fig. 1. So far, there has been no such spectrometer in the pool of instruments at the Nuclear Physics Laboratory at UoA and AMESOS is expected to significantly expand the in–house research program in environmental radiation studies. The technical aspects of the spectrometer and its full characterization prior to field deployment are described later in the text. As a proof of good operation in the field, *AMESOS* was used to measure the natural radioactivity levels in the UoA Zografou Campus, the largest university campus in Greece, hosting ≈70,000 students and staff. To the best of our knowledge this study has been carried out systematically for the first time. The results are presented and discussed in the respective section.

Figure 1. A photo of AMESOS during an in-situ measurement in the UoA campus.

1 the name reflects to the Greek word *ΑΜΕΣΟΣ*: *immediate*, *direct*

Description of the detection apparatus

AMESOS utilizes a 3”×3” NaI(Tl) crystal coupled to an ORTEC digiBASE 14–pin PMT base with integrated bias supply, a preamplifier, and a MCA with digital signal processing (see ref. ORTEC 2020). The digiBASE ensures low power consumption and gain stability, as well as it allows for easy communication with a dedicated portable PC equipped with the MAESTRO32 software via USB. The software enables online analysis, while it also allows for nuclide identification and photopeak integration during the measurement. Typical settings of operation of AMESOS during the field measurements and the lab tests are +700 V for the HV bias, 1024 channels and spectrum energy range ≈ 0–2000 keV.

The detector is placed vertically (Fig. 1), with its end cap facing the ground, inside a custom–made hollow aluminum holder of cylindrical shape (wall thickness is 3 mm), standing on a 3–mm thick plexiglass window mounted firmly at the bottom end of the holder. An additional 3–mm thick lead jacket fills the void space between the detector and the holder and is used as a thin radiation shield from the side. Three removable, extensible legs are mounted on the outer surface of the holder, forming a tripod, which allows for positioning the detector at various heights up to 160 cm from the ground. Horizontal alignment is checked with a bubble meter before starting a measurement. A handheld GPS device is used to track the exact coordinates of the setup for each measurement. The whole apparatus is lightweight and can be easily carried around in a backpack or a carriage.

Recorded spectra can be analyzed offline with the specialized software codes SPECTRW (Kalfas et al. 2016) and XSA (Kumbartzki 2018). In such a configuration, the laptop’s power autonomy is the only potential limiting factor of *AMESOS* operation, which can be overcome easily if long–life battery packs or solar cells are used. During operation, each measurement in the field was performed for a time interval of ≈3 h, which was proven sufficient to run without any power outage interruptions.

Characterization of the spectrometer

Prior to field deployment, the spectrometer was fully studied in terms of its calibration, linearity, energy resolution and absolute efficiency. Separate sets of measurements were carried out to study these properties, as described below.

Lacking an extended–area radionuclide standard, such as those offered by IAEA (IAEA 1987), the calibration was carried out using point sources available at the UoA Nuclear Physics Laboratory. Three standard point sources of known activities, i.e. ^{22}Na (511 and 1274.54 keV), ^{60}Co (1173.23 and 1332.49 keV), and ^{137}Cs (661.66 keV) (Dulieu et al. 2017), were individually placed directly below the detector at point "O" (see Fig. 2). The detector was place at a height h = 1.60 m from the ground.

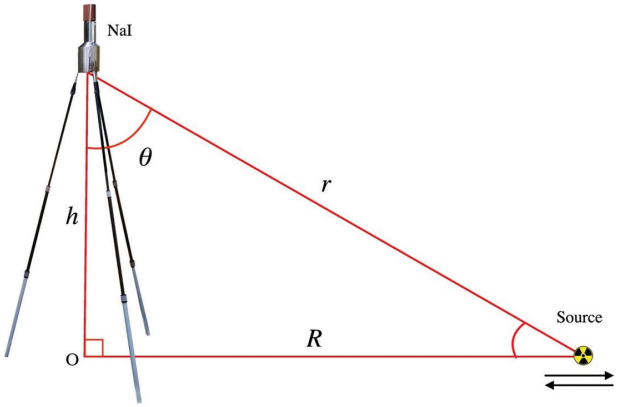

Figure 2. A rough sketch of the experimental setup with AMESOS detecting radiation emitted from a potential source on the ground at a random distance r away from the detector. For the present study, the point sources were placed on the ground, exactly at the point "O".

Spectra for each source were collected for approximately one hour in this series of measurements. The first step in characterizing the spectrometer was to perform an energy calibration and check on its linearity. For the calibration, besides the five photopeaks from the sources, two additional summing peaks (1785.54 keV / ^{22}Na and 2505.72 keV / ^{60}Co, respectively) were used, reaching the typical energy range needed for environmental radioactivity studies (up to ≈3000 keV). The energy values of the photopeak centroids are plotted in Fig. 3a as a function of the respective channel numbers recorded in the raw spectra. A 2nd–order polynomial function was used to fit the data and test *AMESOS* linearity. The fitting curve is also shown in Fig. 3a. The parameters a_0, a_1 and a_2 of the fitting function:

$$E = a_0 + a_1 * (chn) + a_2 * (chn)^2 \quad (1)$$

with (chn) being the channel number, are shown in Table 1. The value of a_2 is very small, reflecting on the good linearity of the spectrometer in the selected energy range. From the same spectra, the energy resolution of the detector was determined in terms of the full width at half maximum (FWHM) as a function of photopeak energy, E. The experimental data are shown in Fig. 3b together with a fitted 2nd–order polynomial function of the form:

$$h(E) = c_0 + c_1 E + c_2 E^2 \quad (2)$$

An overall good fit was produced resulting in the parameter values shown in Table 1.

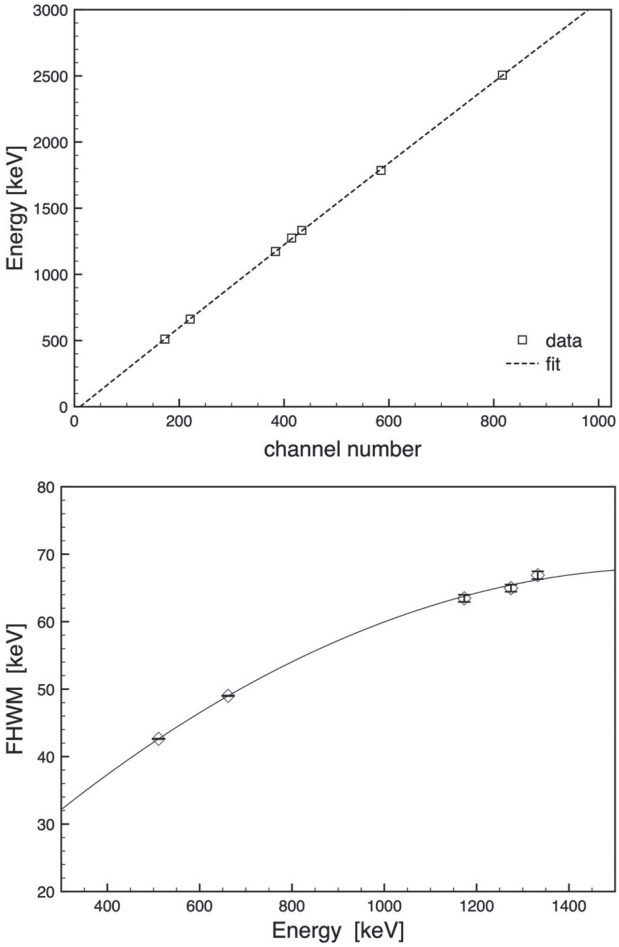

Figure 3. (top) The energy calibration data for AMESOS and the corresponding fit using eq. (1). A good linear response is apparent; (bottom) The FWHM as a function of energy. The solid line is a 2nd–order polynomial fit to the data using eq. (2).

Table 1. Values of the fitted parameters for eq. 1 (top rows), eq. 2 (mid rows), and eq. 4 (bottom rows), respectively

	Parameter	Fitted value
	a_0	34.5 keV
Energy calibration eq. (1)	a_1	3.181 keV chn^{-1}
	a_2	-8.9 × 10^{-5} keV chn^{-2}
	c_0	14.14 keV
Energy resolution eq. (2)	c_1	0.066
	c_2	-2.03 × 10^{-5} keV^{-1}
	b_0	0.6781
Detector efficiency eq. (4)	b_1	0.003184 keV^{-1}
	b_2	0.1352

Further, the absolute efficiency, $\varepsilon(E)$, of the spectrometer was further deduced, using equation (Gilmore 2008, El Khatib et al. 2016, 2017):

$$\varepsilon = \frac{N_{\text{meas}}}{N_o P_\gamma} \tag{3}$$

where N_{meas} is the measured counting rate of the detector for a particular γ–ray photopeak of energy E, corrected for dead time (less that 0.1% throughout the measurements); N_o is the γ–ray emission rate from the source, and P_γ is the relative emission probability of a particular γ–ray with energy E. Uncertainties include the statistical error from the counting rate, the uncertainty of P_γ found in evaluated nuclear databases (Dulieu et al. 2017), and a 3% relative error in the initial activity of the calibration sources, as provided by the manufacturer. Experimental data points are plotted as a function of energy to extract the absolute efficiency of the detector (Fig. 4).

The efficiency data were fitted with Eq. (4), a simplified version of Eq. (1) in McNelles and Campbell (1973). The results are shown as a function of energy E (in keV) in Fig. 4.

$$f(x) = b_0 * e^{-b_1 E} + b_2 \tag{4}$$

The resulted values of the fit parameters are also shown in Table 1.

A final step before field deployment is finding the correspondence between the recorded photopeak counting rate (counts per second, cps) to spatial activity [Bq m^{-2}]. For this task, a circular area of uniform surface distribution with a radius of approximately 2.4 m can be assumed as the source for *all* counts registered in the detector, for the particular height used in the present study (h = 1.6 m). This radius value has been found by extrapolating the results by Billings et al. (2003). Using a source area of $S = \pi R^2 = 18.25$ m^2, all activities measured in AMESOS can now be converted to spatial activities.

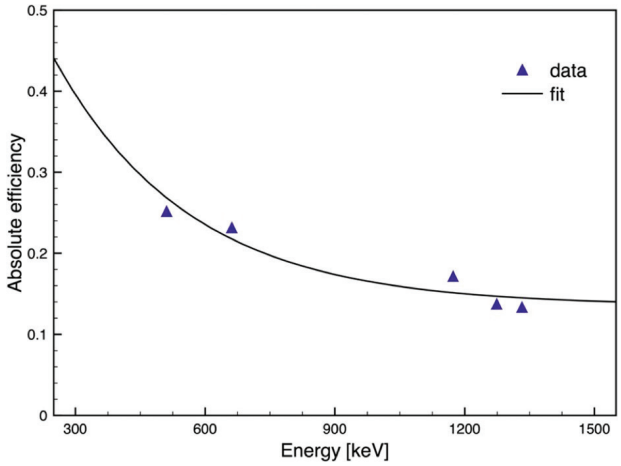

Figure 4. Absolute efficiency of the AMESOS spectrometer as a function of photopeak energy. Uncertainties result in error bars smaller than the symbols (solid triangles). The continuous line represents the best fit to the experimental data, using eq. (4).

Field measurements

After characterizing the spectrometer, a series of measurements were performed in the field. As a proof of good operation, *AMESOS* was deployed on the premises of the metropolitan Zografou campus of UoA. The metropolitan campus covers the largest area among university campuses in Greece and hosts about 65,000 students and 3,000 personnel on a daily basis (UoA 2020). The campus is located at the western foot of Mt. Hymettus in Athens and has a large percentage of undisturbed land covered by grass, bushes and trees. (Fig. 5). The area mainly consists of a) limestones aged Upper Cretaceous (Cenomanian), which are intensely fissured and traversed by a dense and chaotic network of secondary calcite veins infused with

Figure 5. An aerial map of the metropolitan Zografou Campus with the locations of in situ measurements with AMESOS. The dashed line grossly marks the campus borders.

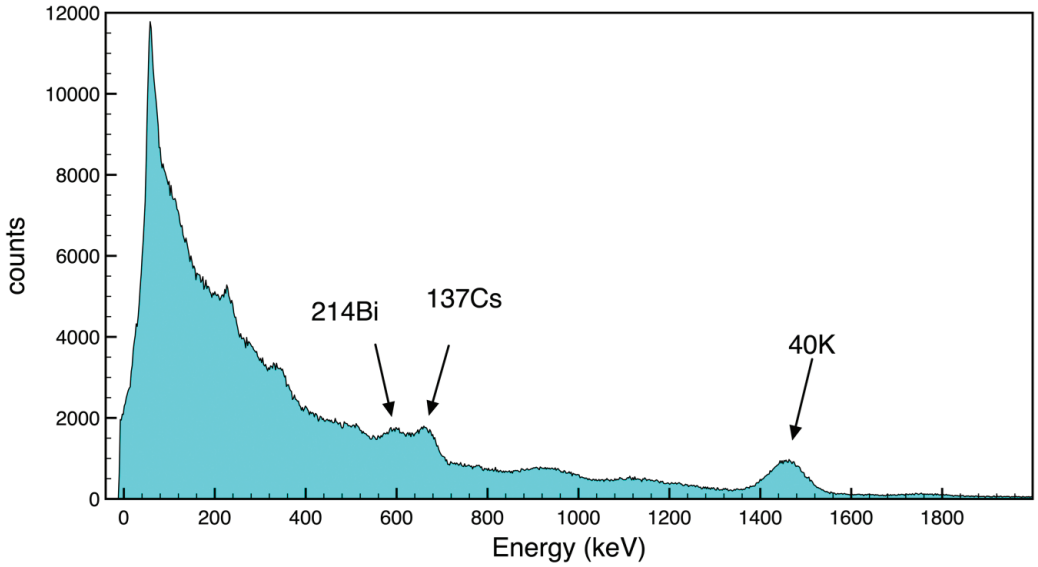

Figure 6. A typical spectrum collected from location ca14. The 609-keV line of ^{214}Bi, the 662-keV line of ^{137}Cs, and the 1461-keV line of ^{40}K, are indicated by the arrows.

Fe-oxides, b) Pleistocene terrestrial and fluvial-terrestrial deposits of various lithological composition (IGME 1996). To the best of our knowledge, a systematic study of the natural radioactivity levels has never been performed on its premises, providing additional motivation to deploy AMESOS at several locations and create radiological maps of naturally occurring radioactive materials (NORM), and of persisting ^{137}Cs concentrations –if any– due to the Chernobyl fallout in 1986.

In situ measurements were performed at twenty (20) different locations of the campus, marked on the campus map shown in Fig. 5. Undisturbed forest lands, as well as parking lots, building backyards etc, were selected as measurement locations, so as to obtain a representative radiological map of the area in the end. A typical spectrum is shown in Fig. 6. The duration of measurement was kept at $\Delta t \approx 3$ h per location. The corresponding GPS coordinates are shown in Table 2 together with the corresponding spatial activities for ^{226}Ra, ^{40}K and ^{137}Cs. All data were combined further to construct radiological maps.

The distribution maps for ^{226}Ra, ^{40}K and ^{137}Cs are shown in the Fig. 7 top, middle and bottom panels, respectively. ^{226}Ra content is estimated from its daughter nucleus ^{214}Bi, which has a half-life of $t_{1/2}$ = 19.8(1) min and is one of the most important γ emitters in the ^{238}U decay chain. In this study, it has been assumed in secular equilibrium with the longer lived ^{226}Ra ($t_{1/2}$ = 1600(7) a). The ^{226}Ra spatial activities are in the range of 0.240–0.749 kBqm^{-2} with a weighted average value of 0.478(2) kBqm^{-2}.

The spatial activity of ^{40}K falls between the values of 4.64 kBqm^{-2} and 13.87 kBqm^{-2} with a weighted average value of 7.10(1) kBqm^{-2}, which is in fair agreement with a reported value of 9.5(3) kBqm^{-2} (Vosniakos et al. 1997) and others (Anagnostakis et al. 1996, Clouvas et al. 2004). Early studies of potassium in Earth's crust report spatial concentrations of ^{40}K ranging 0.51–15 kBqm^{-2} (Eisenbud 1973), in good agreement with the present results.

On the other hand, measurable ^{137}Cs activities have been recorded in only half of the locations studied, all being locations with undisturbed soils. It is known that soon after fallouts, radiocesium is trapped in the top layer of soils and sediments at depths not exceeding 5 cm (Fawaris and Johanson 1995, Isaksson and Erlandsson 1995, Ioannides et al. 1996, Giannakopoulou et al. 2012, Kato et al. 2012).

Table 2. Spatial concentrations in kBq m^{-2} for NORM ^{226}Ra, ^{40}K and the artificially produced ^{137}Cs at the various locations measured in the present study. ^{226}Ra was extracted from its daughter ^{214}Bi. Half of the locations showed no ^{137}Cs distribution (marked as bdl –below detection limit). The experimental uncertainties (shown in parentheses) reflect on the statistical error of the counting rate. All locations are forest/park/low-vegetation areas except those marked with (*) which correspond to parking lots.

Location	Latitude and Longitude	^{226}Ra	^{40}K	^{137}Cs
		[kBqm^{-2}]	[kBqm^{-2}]	[kBqm^{-2}]
ca01	37°58'04.86"N, 23°46'54.66"E	0.562(16)	10.42(9)	bdl
ca02*	37°58'01.02"N, 23°47'05.22"E	0.749(16)	10.18(8)	bdl
ca03	37°58'08.64"N, 23°46'59.76"E	0.240(10)	4.82(6)	0.146(4)
ca04*	37°58'00.66"N, 23°47'14.70"E	0.632(09)	5.20(6)	0.215(5)
ca05	37°57'56.46"N, 23°47'12.12"E	0.737(11)	6.20(8)	0.211(6)
ca06	37°58'17.04"N, 23°45'37.50"E	0.360(11)	6.33(6)	bdl
ca07	37°58'10.32"N, 23°46'42.24"E	0.585(15)	7.97(8)	bdl
ca08	37°58'02.10"N, 23°46'45.84"E	0.409(14)	7.22(7)	bdl
ca09	37°57'57.28"N, 23°46'34.22"E	0.398(08)	4.87(5)	0.374(7)
ca10	37°58'04.32"N, 23°46'35.16"E	0.339(08)	5.50(5)	0.298(7)
ca11	37°58'05.82"N, 23°46'49.92"E	0.347(08)	4.65(6)	0.403(7)
ca12*	37°58'05.28"N, 23°47'12.24"E	0.509(14)	7.72(7)	bdl
ca13	37°58'02.34"N, 23°46'29.40"E	0.509(14)	7.79(7)	bdl
ca14	37°58'04.38"N, 23°46'13.62"E	0.505(10)	11.49(8)	0.511(9)
ca15	37°58'25.80"N, 23°45'41.34"E	0.459(16)	9.56(8)	bdl
ca16	37°58'03.10"N, 23°46'02.28"E	0.637(11)	12.89(9)	bdl
ca17	37°58'07.38"N, 23°46'23.16"E	0.273(11)	5.32(7)	0.359(7)
ca18	37°58'12.48"N, 23°45'56.28"E	0.675(14)	13.87(11)	0.391(7)
ca19	37°57'58.27"N, 23°46'25.39"E	0.472(10)	8.70(6)	bdl
ca20	37°57'58.76"N, 23°46'50.25"E	0.638(17)	7.11(6)	0.314(6)

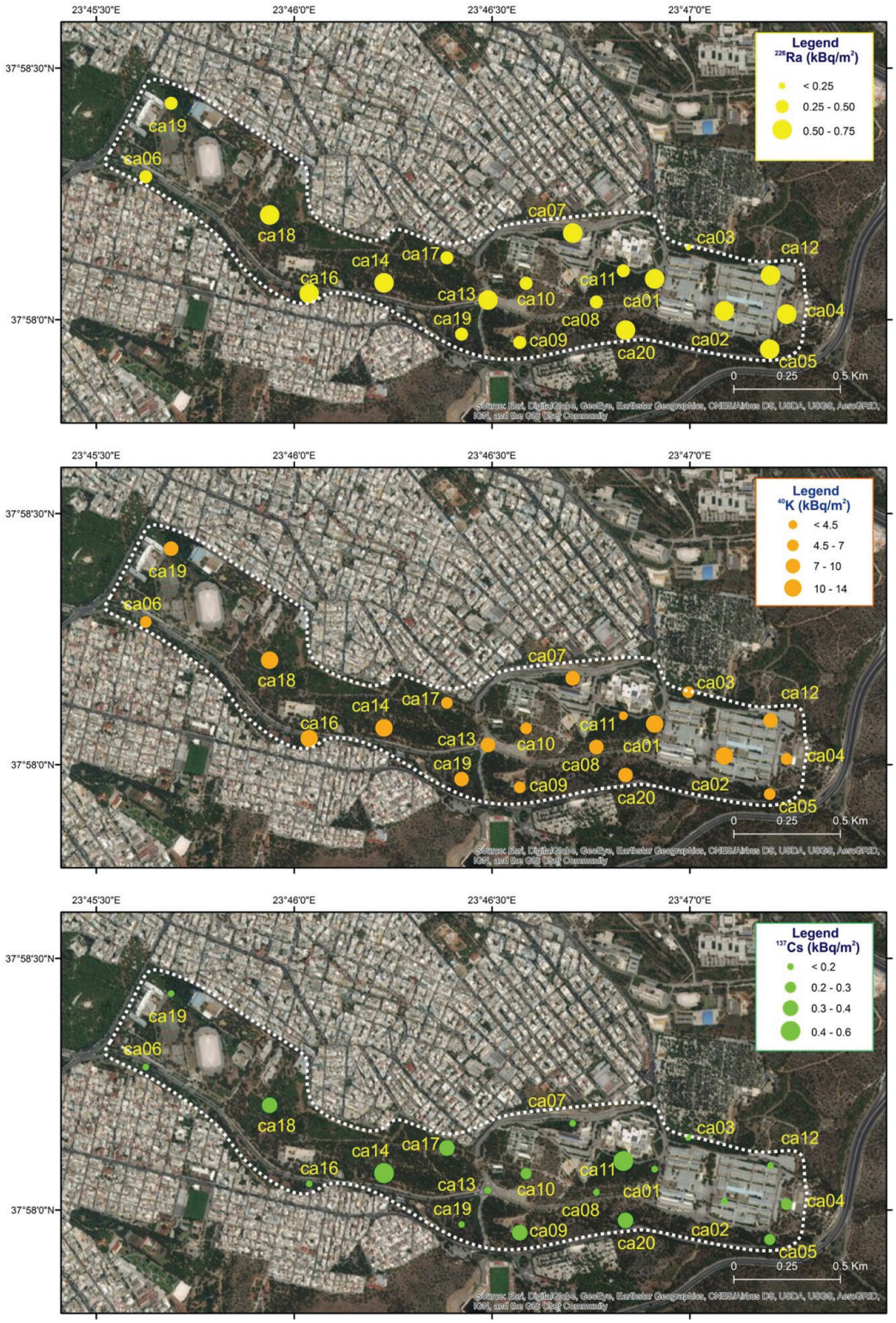

Figure 7. Radiological maps of ^{226}Ra (top), ^{40}K (middle) and ^{137}Cs (bottom).

Besides the natural decay of radiocesium, any source of soil disturbance may result in additional reduction of ^{137}Cs activity. An additional motivation behind the initial plan to deploy AMESOS in UoA was to target such undisturbed soils, in an attempt to study the persistence of Chernobyl fallout in soils of Athens and elsewhere. Athens with its neighboring suburbs form a megacity of 5 million people, where undisturbed land is nowadays rare to find and study in terms of the long–term impact of man–made radioactivity. In that aspect, the metropolitan UoA campus is a great natural lab to assess the situation, almost 35 years after the 1986 Chernobyl fallout in Greece.

The ^{137}Cs values are significantly lower than those recorded in Athens immediately after Chernobyl (Simopoulos 1989, Kritidis et al. 1990) or later (Kritidis and Florou 1995, Anagnostakis et al. 1996, Petropoulos et al. 1996), showing a significant reduction of its retention in soils. The present ^{137}Cs measurements fall in the range 0.211–0.511 kBqm^{-2} and are ≈20 times lower than the average value of 9.0 kBqm^{-2} in Greek soils reported in 1990 by (Kritidis et al. 1990) and ≈10 times lower than the average 4.0(2) kBqm^{-2} reported for Attica prefecture 10 years after Chernobyl fallout (Vosniakos et al. 1997). The reduction may be attributed to environmental processes, other than the natural decay of radiocesium, such as soil erosion, surface runoff, migration to deeper soil layers and plant root uptake (Kritidis and Florou 1995, Arapis and Karandinos 2004). This reduction is also in agreement with recent studies of undisturbed soils in locations of Northern Greece (Mertzimekis et al. 2014) where the Chernobyl fallout peaked in Greece (Simopoulos 1989, Kritidis et al. 1990, ICRU 1994, Kritidis and Florou 1995, Vosniakos et al. 1997, Arapis and Karandinos 2004, Clouvas et al. 2004).

Conclusions

A mobile spectrometer, *AMESOS*, was developed and characterized at the University of Athens to be used for environmental radioactivity studies. The spectrometer was found to behave well during field operation performing γ–ray spectroscopic studies. The first application of the spectrometer focused on assessing the NORM distributions (^{226}Ra and ^{40}K) in the National and Kapodistrian University of Athens Zografou campus for the first time. In addition to the NORM levels, the man–made ^{137}Cs levels were examined in the studied locations and were found above detection limits in half of them. Despite the respective areal concentrations are small, the effects of the Chernobyl fallout for more than 30 years in the undisturbed soils of Athens seem to persist. Based on the measurements, a set of radiological maps were constructed for the UoA campus to serve as reference for future studies in the area. Overall, the deployment of *AMESOS* in the field can be considered successful. The mobile spectrometer will be further used for both research and educational purposes in the near future.

Data availability statement

Raw gamma-ray spectra collected during this research are openly available at: https://doi.org/10.6084/m9.figshare.14794449. All other derived data are available from the corresponding author on reasonable request.

Acknowledgements

The authors would like to thank Ms. Martha Costos for improving the language of the manuscript. This work is partially supported by RAMONES, funded by the European Union's Horizon 2020 research and innovation programme, under grant agreement No 101017808.

References

- Anagnostakis M, Hinis E, Simopoulos S, Angelopoulos M (1996) Natural radioactivity mapping of greek surface soils. Environment International 22, Supplement 1: 3–8. [the Natural Radiation Environment VI] https://doi.org/10.1016/S0160-4120(96)00085-2
- Androulakaki E, Tsabaris C, Eleftheriou G, Kokkoris M, Patiris D, Pappa F, Vlastou R (2016) Efficiency calibration for in situ γ–ray measurements on the seabed using Monte Carlo simulations: Application in two different marine environments. Journal of Environmental Radioactivity 164: 47–59. https://doi.org/10.1016/j.jenvrad.2016.06.015
- Arapis GD, Karandinos MG (2004) Migration of ^{137}Cs in the soil of sloping semi–natural ecosystems in northern Greece. Journal of Environmental Radioactivity 77: 133–142. https://doi.org/10.1016/j.jenvrad.2004.03.004
- Billings SD, Minty BR, Newsam GN (2003) Deconvolution and spatial resolution of airborne gamma-ray surveys. Geophysics 68: 1126–1422. https://doi.org/10.1190/1.1598118
- Clouvas A, Xanthos S, Antonopoulos-Domis M (2004) Radiological maps of outdoor and indoor gamma dose rates in Greek urban areas obtained by in situ gamma spectrometry. Radiation Protection Dosimetry 112(2): 267–275. https://doi.org/10.1093/rpd/nch395
- Cresswell AJ, Sanderson DCW, Harrold M, Kirley B, Mitchell C, Weir A (2013) Demonstration of lightweight gamma spectrometry systems in urban environments. Journal of Environmental Radioactivity 124: 22–28. https://doi.org/10.1016/j.jenvrad.2013.03.006
- Cresswell AJ, Sanderson DCW, Yamaguchi K (2018) Assessment of the calibration of gamma spectrometry systems in forest environments. Journal of Environmental Radioactivity 181: 70–77. https://doi.org/10.1016/j.jenvrad.2017.10.019
- Dulieu C, Kellett MA, Mougeot X (2017) Dissemination and visualisation of reference decay data from decay data evaluation project (DDEP). EPJ Web Conf. 146: 07004. https://doi.org/10.1051/epjconf/201714607004
- Eisenbud M (1973) Environmental Radioactivity. Academic Press, New York.
- El-Khatib AM, Badawi MS, Thabet AA, Jovanovic SI, Gouda MM, Mohamed MM, Dlabac AD, Abd-Elzaher M, Mihaljevic NN, Abbas MI (2016) Well–type NaI(Tl) detector efficiency using analytical technique and ANGLE4 software based on radioactive point sources located out the well cavity. Chinese Journal of Physics 54: 338–346. https://doi.org/10.1016/j.cjph.2016.03.019
- El-Khatib AM, Salem BA, Badawi MS, Gouda MM, Thabet AA, Abbas MI (2017) Full–energy peak efficiency of an NaI(Tl) detector with coincidence summing correction showing the effect of the source–to–detector distance. Chinese Journal of Physics 55: 478–489. https://doi.org/10.1016/j.cjph.2016.11.013

- Fawaris B, Johanson K (1995) A comparative study on radiocaesium (^{137}Cs) uptake from coniferous forest soil. Journal of Environmental Radioactivity 28: 313–326. https://doi.org/10.1016/0265-931X(95)97302-S
- Giannakopoulou F, Gasparatos D, Haidouti C, Massas I (2012) Sorption behavior of cesium in two Greek soils: Effects of cs initial concentration, clay mineralogy, and particle-size fraction. Soil and Sediment Contamination: An International Journal 21: 937–950. https://doi.org/10.1080/15320383.2012.714418
- Gilmore GR (2008) Practical Gamma–ray Spectrometry. 2nd edn. Wiley. https://doi.org/10.1002/9780470861981
- Hattori M (2000) Sea bottom γ–ray measurement by NaI(Tl) scintillation spectrometer installed on manned submersibles, ROV and sea bottom long–term observatory. Proceedings of the 2000 International Symposium on Underwater Technology 2000.
- Hattori M, Okano M (2001) New results of sea bottom radioactivity measurement. JAMSTEC J. Deep Sea Research 18: 1–13. https://ci.nii.ac.jp/naid/10020374222/en/ [in Japanese with English abstract]
- IAEA (1987) IAEA Report AL/148. [Online] https://nucleus.iaea.org/rpst/Documents/rl148.pdf
- ICRU (1994) Gamma-ray spectrometry in the environment (ICRU report 53).
- IGME (1996) Hellenic Survey of Geology and Mineral Exploration, Geological Map of Greece, Koropi-Plaka Sheet, 1:50000
- Ioannides KG, Mertzimekis TJ, Karamanis DT, Stamoulis KC, Kirikopoulos I (1996) Radiocesium sorption–desorption processes in lake sediments. Journal of Radioanalytical and Nuclear Chemistry 208: 549–557. https://doi.org/10.1007/BF02040072
- Isaksson M, Erlandsson B (1995) Experimental determination of the vertical and horizontal distribution of ^{137}Cs in the ground. Journal of Environmental Radioactivity 27: 141–160. https://doi.org/10.1016/0265-931X(95)00017-5
- Jilek T, Zalud L, Kocmanova P (2016) Robotic autonomous outdoor gamma radiation monitoring and mapping. International Journal of Systems Applications, Engineering & Development 10: 162–168.
- Kalfas C, Axiotis M, Tsabaris C (2016) SPECTRW: A software package for nuclear and atomic spectroscopy. Nuclear Instruments and Methods in Physics Research Section A: Accelerators, Spectrometers, Detectors and Associated Equipment 830: 265–274. https://doi.org/10.1016/j.nima.2016.05.098
- Kato H, Onda Y, Teramage M (2012) Depth distribution of ^{137}Cs, ^{134}Cs, and ^{131}I in soil profile after Fukushima Dai-ichi nuclear power plant accident. Environmental Impacts of the Fukushima Accident (Part I). Journal of Environmental Radioactivity 111: 59–64. https://doi.org/10.1016/j.jenvrad.2011.10.003
- Kock P, Samuelsson C (2011) Comparison of airborne and terrestrial gamma spectrometry measurements – evaluation of three areas in southern Sweden. Journal of Environmental Radioactivity 102: 605–613. https://doi.org/10.1016/j.jenvrad.2011.03.010
- Kritidis P, Florou H (1995) Environmental study of radioactive caesium in Greek lake fish after the Chernobyl accident. Journal of Environmental Radioactivity 28: 285–293. https://doi.org/10.1016/0265-931X(95)97300-2
- Kritidis P, Florou H, Papanicolaou E (1990) Delayed and late impact of the Chernobyl accident on the Greek environment. Radiation Protection Dosimetry 30: 187–190. https://doi.org/10.1093/oxfordjournals.rpd.a080617
- Kumbartzki G (2018) XSA: A spectrum analysis program (unpublished). http://www.physics.rutgers.edu/~kum/sa.html
- Kurvinen K, Smolander P, Pöllänen R, Kuukankorpi S, Kettunen M, Lyytinen J (2005) Design of a radiation surveillance unit for an unmanned aerial vehicle. Journal of Environmental Radioactivity 81: 1–10. https://doi.org/10.1016/j.jenvrad.2004.10.009
- Mertzimekis TJ, Ioannidis I, Godelitsas A, Gasparatos D, Stamoulis K, Ioannides K (2014) Assessing Chernobyl's impact on Central Greece soils: a study overtaken a radiocesium halflife later. In: EGU General Assembly. p. id.7817.
- ORTEC (2020) digiBASE A Technical Manual. AMETEK/ORTEC. http://www.ortec-online.com/-/media/ametekortec/manuals/digibase-mnl.pdf
- Petropoulos NP, Hinis EP, Simopoulos SE (1996) ^{137}Cs Chernobyl fallout in Greece and its associated radiological impact. Environment International 22, Supplement 1: 369–373. [the Natural Radiation Environment VI] https://doi.org/10.1016/S0160-4120(96)00133-X
- Pöllänen R, Toivonen H, Peräjärvi K, Karhunen T, Ilander T, Lehtinen J, Rintala K, Katajainen T, Niemelä J, Juusela M (2009) Radiation surveillance using an unmanned aerial vehicle. Applied Radiation and Isotopes 67: 340–344. https://doi.org/10.1016/j.apradiso.2008.10.008
- Simon SL, Graham JC (1998) A comparison of aerial and ground level measurements of ^{137}Cs in the Marshall Islands. Environmental Monitoring and Assessment 53: 363–377. https://doi.org/10.1023/A:1005876130072
- Simopoulos SE (1989) Soil sampling and ^{137}Cs analysis of the Chernobyl fallout in Greece. International Journal of Radiation Applications and Instrumentation. Part A. Applied Radiation and Isotopes 40: 607. https://doi.org/10.1016/0883-2889(89)90116-0
- Tsabaris C, Patiris D, Lykousis V (2011) KATERINA: An in-situ spectrometer for continuous monitoring of radon daughters in aquatic environment. Nuclear Instruments and Methods in Physics Research, Section A 626–627(Suppl.): S142–S144. https://doi.org/10.1016/j.nima.2010.06.233
- UOA (2020) National and Kapodistrian University of Athens, official website. http://www.uoa.gr
- Vosniakos F, Zoumakis N, Diomou C (1997) The level of ^{137}Cs concentration in Greek soils one decade after the Chernobyl accident. In: IAEA–TECDOC–964 / One Decade after Chernobyl: Summing Up the Consequences of the Accident. Vol. 2. IAEA.